Dilepton decay from excited states in ^{28}Si populated via different isospin entrance channels

A. Buda, J. C. Bacelar, A. Bałanda,* A. Krasznahorkay,† H. van der Ploeg, Z. Sujkowski,‡ and A. van der Woude
Kernfysisch Versneller Instituut, 9747AA Groningen, The Netherlands

(Received 14 July 1995)

Nuclear states in ^{28}Si, with an initial excitation energy $E^*=50$ MeV, were populated via the isospin $T=0$ reaction ^{4}He+^{24}Mg and the mixed-isospin ^{3}He+^{25}Mg reaction. In both reactions the dilepton (e^+e^-) and photon decay yields were measured concurrently, up to transition energies of 30 MeV. Both the dilepton and the photon yields are well described by a modified version of the statistical decay model, which includes both the photon and dilepton decays of giant resonances built on excited nuclear states. An excess of counts in the e^+e^- spectrum, over the converted photon yield, is observed in the energy region 17–22 MeV in the ^{3}He induced reaction, possibly indicating an entrance channel effect.

PACS number(s): 24.30.Cz, 23.20.Ra, 25.55.−e, 27.30.+t

I. INTRODUCTION

The electromagnetic decay of excited states of a nucleus proceeds either by direct photon emission or by one of several internal conversion modes. Internal-pair creation ($\alpha_\pi = P_{e^+e^-}/P_\gamma$) increases with the transition energy and is largest for low multipolarities [1], while internal K-electron conversion ($\alpha_K = P_{e^-}/P_\gamma$) decreases with energy and is largest for high multipolarity. On the other hand, the dependence upon the nuclear charge (Z) of pair emission [1] is rather weak for $Z<137$, whereas it is strong for electron conversion [2]. In case of an $E1$ transition $\alpha_\pi/\alpha_K>1$ for energies above 2 MeV. At about 10 MeV, $\alpha_\pi(E1)\approx 3\times 10^{-3}$ and it is three ($Z\approx 20$) to one ($Z\approx 100$) order of magnitude greater than α_K.

Internal conversion modes are important particularly for the measurements of electric monopole ($E0$) transitions [3]. A very special feature of $E0$ transitions is the absence of single-photon emission, because a photon must carry at least one unit of angular momentum. Therefore, electromagnetic monopole transitions predominantly occur by bound-state electron conversion or by internal positron-electron pair creation. The e^+e^- dominance can be striking for high-energy transitions: $P_{e^+e^-}/P_{e_K}$ is as large as 2.6×10^4 for the $E0$ transition from the 6.05 MeV 0^+ state to the ground state in ^{16}O. This makes internal pair creation a suitable tool to measure electromagnetic $0^+\rightarrow 0^+$ decays. It has in the past been successfully applied to search for excited 0^+ states [3].

$E0$ transitions are extremely sensitive to changes in the nuclear charge distribution. Actually they correspond to the expansion and compression of the charge distribution which does not affect the electromagnetic field outside the nuclear volume since there the monopole moment is constant. This shows that the measurement of dilepton decay is interesting to investigate properties of giant monopole resonances (GMR). Of course, one has to be aware of the fact that the expected relative decay probability for e^+e^- is only of the order of 10^{-6} compared to particle decay [4], therefore requiring very careful exclusive measurements.

The existence of the isoscalar giant monopole resonance (ISGMR), the so-called breathing mode, has been well established already for many years [5]. The ISGMR is of particular interest due to its bearing with the compressibility of nuclei [6,7] and hence to the compressibility of nuclear matter [8,9]. The latter quantity is one of the key ingredients, like the saturation density and the binding energy per nucleon, of the equation of state (EOS) of nuclear matter.

The most commonly used probe in ISGMR studies is inelastic scattering at 0° [5,8–12]. This and other methods used so far to excite the ISGMR constrains such studies to ground-state excitations. The hypotheses of Brink [13], that a giant resonance can be built upon each excited nuclear state with properties that would be largely independent of the detailed microscopic structure of this excited state, allows one to study the nuclear temperature dependence of the GR's strength distribution. The Brink hypothesis has been tested extensively for the isovector giant dipole resonance (IVGDR) [14,15].

It is therefore interesting to extend the experimental studies of the properties of the ISGMR to (hot) nuclear excited states in the hope to deduce the dependence of the nuclear compressibility on temperature. Recent calculations [16] predict only a small temperature dependence of the compressibility, which decreases by about 10% from 0 to 4 MeV temperature. Similarly to the studies of the IVGDR, the ISGMR in hot nuclei can be populated in compound fusion reactions [17–19]. The studies of the statistical decay of the ISGMR built on excited nuclear states call for a novel and sensitive detection method. The measurement of the e^+e^- pair-decay yield coupled to specific reaction channels, is the method suggested in this work and the results of the first experiments are discussed. Preliminary reports are given in [20,21].

The experimental data on dilepton decay presented here were obtained by measuring the decay of ^{28}Si formed in fusion-evaporation reactions. Section II describes a modified version of the statistical-model code CASCADE [22] which

*Permanent address: Institute of Physics, Jagellonian University, Cracow, 30-059 KraKow, Reymonta 4, Poland.
†Permanent address: Nuclear Research Institute of the Hungarian Academy of Sciences, Debrecen, Hungary.
‡Permanent address: Soltan Institute for Nuclear Studies, Swierk, Poland.

includes e^+e^- yields resulting from the internal-pair-creation (IPC) processes. A novel positron-electron pair spectroscopy instrument (PEPSI), which has been designed for studying the emission of positron-electron pairs in the energy range 10–40 MeV, is described briefly in Sec. III. A detailed description of this spectrometer can be found elsewhere [23]. The results of the first measurement of the internal pair conversion coefficient for the sharp 15.1 MeV $M1$ transition in ^{12}C are also given. In Sec. IV the dilepton- and photon-yield measurements following the ^{4}He+^{24}Mg reaction (at E_α=48 MeV) with an entrance channel isospin T=0 and the ^{3}He+^{25}Mg reaction (at $E_{^3\mathrm{He}}$=31 MeV) with a mixed T=0 and T=1 for the populated compound states are discussed. Both reactions populate initial states in the compound nucleus ^{28}Si at an excitation energy of about 50 MeV. Dilepton and photon yields from the two reactions are compared in order to look for the weak isoscalar $E0$ strength, which should be relatively enhanced over the IVGDR in the case of the isospin T=0 compound-fusion entrance channel. Finally a summary is presented in Sec. V.

II. GIANT RESONANCES IN THE STATISTICAL MODEL

A. Modified CASCADE code description

1. Inclusion of isospin

The compound system can decay statistically not only by evaporation of particles (predominantly neutrons) but also by emission of γ rays. The γ-decay rate is given by [14]

$$R_\gamma dE_\gamma=\frac{1}{\hbar}\,\Gamma_\gamma(E_\gamma)=\frac{\rho_f(E_f,J_f,\pi_f)}{2\pi\hbar\rho_i(E_i,J_i,\pi_i)}\sum_L F_\gamma^L(E_\gamma)dE_\gamma, \tag{1}$$

$$F_\gamma^L(E_\gamma)dE_\gamma=2\pi\hbar P_\gamma^L(E_\gamma), \tag{2}$$

where L denotes the multipolarity of the γ ray, $F_\gamma^L(E_\gamma)$ are energy-dependent strength functions, and $P_\gamma^L(E_\gamma)$ are γ-emission probabilities. The nuclear level densities, at specific excitation energy (E), spin (J), and parity (π), are given by the functions $\rho(E,J,\pi)$.

Although electromagnetic transitions cannot change $\mathbf{T}_z=(N-Z)/2$, they can proceed with a change of isospin $\mathbf{T}$. Therefore, isospin plays an important role in decay yields of giant resonances built on excited states, as was experimentally shown for the isovector giant dipole resonance [24]. The isovector decay will vanish for $\Delta\mathbf{T}=0$ transitions in case of $\mathbf{T}_z=0$ nuclei. Therefore, isospin Clebsch-Gordan coefficients $\langle T^fT_z^f tt_z|T^iT_z^i\rangle$, where $\mathbf{T}^i$ and $\mathbf{T}^f$ are the isospin of the initial and final states, respectively, and t is the isospin of the decay channel, are introduced into the calculation of both, particle and γ-ray decay widths. In this modified version of the CASCADE code [24] the level density for a given excitation energy, in addition to the pairing and rotational energy, is further shifted back by an amount equal to the energy of the isobaric analogue state, for states with $T=T_z+1$.

To account for the isospin mixing, $\mathbf{T}_<=|\mathbf{T}_z|$ and $\mathbf{T}_>=|\mathbf{T}_z+1|$, level densities of the initial states of the compound nucleus are modified according to

$$\tilde\rho(T_<)=(1-\beta^2)\rho(T_<)+\beta^2\rho(T_>),$$

$$\tilde\rho(T_>)=(1-\beta^2)\rho(T_>)+\beta^2\rho(T_<), \tag{3}$$

where $\tilde\rho$ and ρ are the mixed and pure level densities, respectively. β^2 is the isospin mixing parameter [24].

The strength functions $F_\gamma^L(E_\gamma)$ used in Eqs. (1) and (2) are related to the classical energy weighted sum rules (EWSR's) of specific operators. The EWSR for different multipolarities in the isospin-dependent form are given by [25]

$$S(\mathrm{IS}\ E0)=\frac{2\hbar^2}{m_N}\frac{Z^2}{A}\langle r^2\rangle, \tag{4}$$

$$S(\mathrm{IV}\ E1)=\frac{9\hbar^2}{8\pi m_N}\frac{NZ}{A}(1+\kappa), \tag{5}$$

$$S(\mathrm{IS}\ EL)=\frac{L(2L+1)^2\hbar^2}{8\pi m_N}\frac{Z^2}{A}\langle r^{2L-2}\rangle, \tag{6}$$

$$S(\mathrm{IV}\ EL)=\frac{L(2L+1)^2\hbar^2}{8\pi m_N}\frac{NZ}{A}\langle r^{2L-2}\rangle(1+\kappa^L), \tag{7}$$

where $L\geqslant 2$, r is the radius of the nucleus and m_N is the nucleon mass. IS and IV stand for the isoscalar and the isovector transitions, respectively. An extra factor $(1+\kappa^L)$ for the isovector transitions stems from the charge-exchange terms in the nucleon-nucleon interaction [26]. This factor is neglected in the present calculations. Assuming that the energy-weighted transition strength for a multipole L is distributed over the compound states with a Lorentzian distribution, then

$$E|M(EL)|^2\rho(E)dE=C(L)\frac{E^2\Gamma}{(E_0^2-E^2)^2+E^2\Gamma^2}\,dE, \tag{8}$$

where E_0 and Γ are the resonance energy and width, respectively (following the formalism described in [17]). The normalization constant $C(L)$ is obtained by integrating both sides of Eq. (8) over all transition energies from zero to infinity. Combination of Eqs. (2), (5), and (8) yields the strength function for the isovector GDR (i.e., L=1),

$$F_{\mathrm{IVGDR}}(E_\gamma)=\frac{8\alpha}{3m_Nc^2}\frac{NZ}{A}\frac{E_\gamma^4\Gamma_{\mathrm{IVGDR}}}{(E_{\mathrm{IVGDR}}^2-E_\gamma^2)^2+E_\gamma^2\Gamma_{\mathrm{IVGDR}}^2}, \tag{9}$$

where α is the fine-structure constant. In the case of the isoscalar giant quadrupole resonance (ISGQR) we get

$$F_{\mathrm{ISGQR}}(E_\gamma)=\frac{4\alpha}{15(\hbar c)^2}\frac{Z^2}{A}\frac{E_\gamma^6\Gamma_{\mathrm{ISGQR}}}{(E_{\mathrm{ISGQR}}^2-E_\gamma^2)^2+E_\gamma^2\Gamma_{\mathrm{ISGQR}}^2}. \tag{10}$$

The IVGQR strength function is obtained by substituting NZ/A for Z^2/A.

2. Inclusion of dilepton decays

As well as γ-ray decay, positron-electron pairs can also be emitted. For transition multipolarities $L\geqslant 1$, the strength

functions for pair emission are simply the respective γ-strength functions multiplied by the energy- and multipolarity-dependent internal pair conversion coefficients (α_π).

Neglecting penetration effects, i.e., the overlap between the electronic wave function and the nuclear charge density within the nuclear radius, and in the Born approximation (Z small or large transition energy ω), the doubly differential pair conversion coefficient [1], for an electric transition with multipolarity $L \geqslant 1$ is given by

$$\frac{d^2\alpha_\pi^{\mathrm{Born}}(EL)}{dE_+ d\cos\theta} = \frac{2\alpha}{\pi(L+1)} \frac{p_+ p_-}{q} \frac{\left(\frac{q}{\omega}\right)^{2L-1}}{(\omega^2-q^2)^2} \left\{ (2L+1)\left(E_+E_- + 1 - \frac{1}{3} p_+p_- \cos\theta \right) + L\left[\left(\frac{q^2}{\omega^2}\right) - 2 \right](E_+E_- - 1 + p_+p_- \cos\theta) + \frac{1}{3}(L-1)p_+p_- \left[\left(\frac{3}{q^2}\right)(p_- + p_+ \cos\theta)((p_+ + p_- \cos\theta) - \cos\theta) \right] \right\}, \tag{11}$$

where the transition energy $\omega=(E_f-E_i)/m_ec^2$, θ is the opening-angle between the positron and electron, and $\vec{\mathbf{q}}=\vec{\mathbf{p}}_+ + \vec{\mathbf{p}}_-$. The indices + and − are used to label observables for positrons and electrons, respectively.

For the special case of $E0$ transitions, the $E0$ matrix element includes only scalar parts and therefore has a simple form [1]

$$U_{if}^{el}(L=0) = -\alpha \int_0^\infty d\tau_n \int_0^{\tau_n} d\tau_e \rho_n(r_n)\rho_e(r_e)\left[\frac{1}{r_n} - \frac{1}{r_e}\right]. \tag{12}$$

This expression shows that the $E0$ conversion takes place only by penetration effects: i.e., only that part of the electron density which is contained inside the nucleus contributes to the integral. In other words, the characteristic feature of an $E0$ transition is that the interaction between the protons and the lepton pair takes place inside the nuclear volume, and it is therefore sensitive to the nuclear charge distribution.

The doubly differential pair-creation probability was calculated recently by Hofmann *et al.* [27]. Again in the Born approximation (valid for low Z nuclei) it leads to

$$\frac{d^2P_{e^+e^-}^{\mathrm{Born}}}{dE_+ d\cos\theta}(E0) = \frac{\alpha^2}{9\pi}|M|^2 p_+p_-(E_+E_- - 1 + p_+p_- \cos\theta). \tag{13}$$

Following the same procedure as discussed for $L \geqslant 1$ we get for the isoscalar $E0$ strength function with 100% of the EWSR:

$$F_{\mathrm{ISGMR}}(E_{e^+e^-}) = \frac{8\alpha^2}{135\pi(\hbar c)^2} \frac{Z^2}{A} \frac{\langle r^2\rangle}{m_Nc^2} \times \frac{E_{e^+e^-}^6 \Gamma_{\mathrm{ISGMR}}}{(E_{\mathrm{ISGMR}}^2 - E_{e^+e^-}^2)^2 + E_{e^+e^-}^2 \Gamma_{\mathrm{ISGMR}}^2}. \tag{14}$$

The IVGMR strength function is obtained by substituting Z^2/A by NZ/A.

The above strength functions for the e^+e^- decay of the compound nucleus [Eq. (14) for $E0$ strength, and Eqs. (9) and (10), multiplied by Eq. (11) for $E1$ and $E2$ strength, respectively] were included in the modified version of the CASCADE code which treats isospin explicitly.

As an example of the dilepton phase-space distribution for different multipolarities, the doubly differential e^+e^- probabilities for $E0$ and $E1$ transitions of 15.1 MeV are shown in Fig. 1. Since the influence of the Coulomb field is neglected in the Born approximation, the two distributions are symmetric around the line of equal energy sharing ($E_+=E_-$). The striking feature of all distributions with $L \geqslant 1$ (for which the $E1$ is a good example) is the large probability of parallel emission of positron and electron (i.e., with an e^+e^- opening angle close to 0°) in comparison with the flatter $E0$ distribution. In case of an $E0$ transition an emission of particles with equal energies is preferred, whereas the distributions for multipolarities $L \geqslant 1$ are rather uniform (see also Fig. 2). The differences in the energy and opening-angle distributions between, on the one hand, $E0$ and, on the other hand, higher-order transitions (illustrated by the $L=1$ case) can in principle be used as a way to experimentally select monopole decays.

B. Calculations of dilepton yields from ^{28}Si*

The positron-electron pair decay of excited states in ^{28}Si*, with an initial excitation energy of $E^*=50$ MeV, populated by ^{3}He+^{25}Mg and ^{4}He+^{24}Mg compound-nucleus reactions, was studied. The entrance channel isospin is different for the two reactions: $T=0$ for the ^{4}He-induced reaction, and $T=0,1$ for the ^{3}He reaction.

The parameters defining the Lorentzian strength distributions of the different giant resonances are given in Table I. For the IVGDR and the ISGQR, the parameters reported by Harakeh *et al.* [24] were used. These were obtained from γ-ray emission studies from ^{28}Si formed at a somewhat lower excitation energy. The isospin mixing parameter [β^2 in Eq. (3)] was 4.7% [28]. The parameters for the IVGMR were

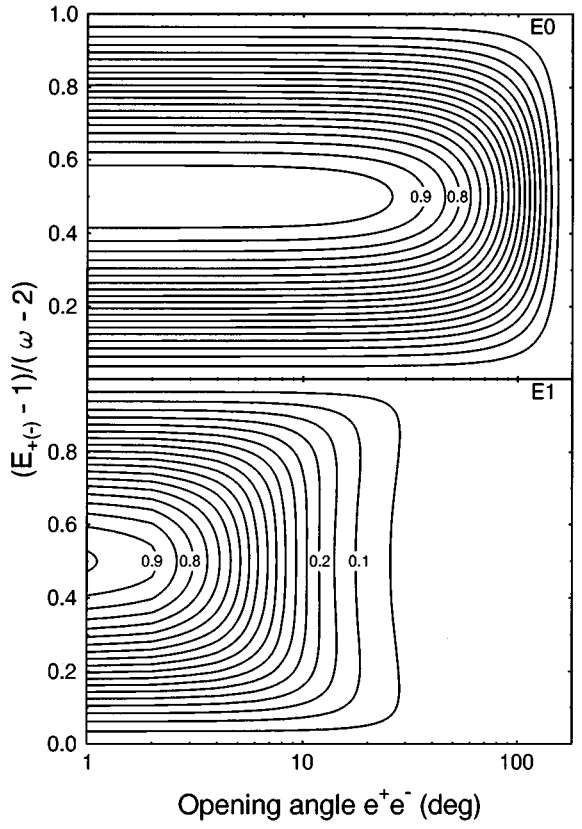

FIG. 1. Energy sharing and opening angle distributions for $E0$ (top) and $E1$ (bottom) transitions of 15.1 MeV, decaying by e^+e^-, calculated in the Born approximation. The contour lines are drawn at intervals representing 5% changes in the probability distribution.

taken from systematics [5] based on the results of charge-exchange ($\pi^{\pm},\pi^0$) experiments [29,30]. In light nuclei, the ISGMR and other resonances built on the ground state are very fragmented. Therefore, there are large ambiguities in

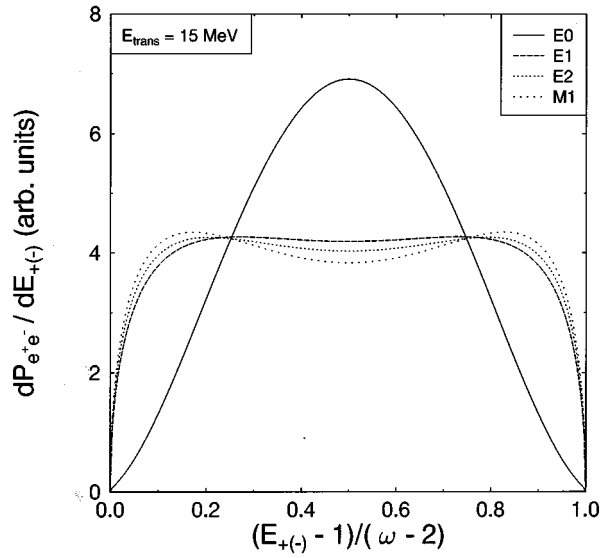

FIG. 2. Energy sharing between the positron and the electron for a transition of 15 MeV, calculated in the Born approximation for different multipolarities.

TABLE I. The parameters of the Lorentzian-shaped giant resonance strength distributions used in the modified statistical model calculations for the decay of ^{28}Si compound nucleus.

Resonance type	Centroid energy (MeV)	Width (MeV)	Fraction of EWSR
ISGMR	22.0	4.8	1.0
IVGMR	34.0	7.0	1.0
IVGDR	20.2	8.8	1.0
ISGQR	17.0	10.0	1.0

determining the GMR parameters. Lui *et al.* [11] measured the excitation of the ISGMR built on the ground state of ^{28}Si by inelastic alpha scattering at 0°. They identified 66% of the $E0$ EWSR with a width (Γ_{ISGMR}) of 4.8 MeV centered (E_{ISGMR}) at 17.9 MeV. Coincidence measurements [31] of charged-particle (proton and alpha) decay of the ISGMR in ^{28}Si are consistent with this result. Systematics of the GMR centroid energy [5] predict for ^{28}Si a centroid energy of $E_{\mathrm{ISGMR}} \sim 22$ MeV.

Figure 3 presents the calculated dilepton energy spectra for electric transitions of different multipolarities for the ^{3}He+^{25}Mg$\rightarrow^{28}$Si* reaction [Fig. 3(a)] and for the ^{4}He+^{24}Mg$\rightarrow^{28}$Si* reaction [Fig. 3(b)]. The entrance channel isospin effect is clearly visible in the $E1$ (IVGDR) strength depicted in this figure. The main contribution to the monopole decay yield comes from $\Delta T=0$ transitions (ISGMR), so there is almost no difference in the $E0$ strength distribution between the two reactions. The same applies for the $E2$ (ISGQR) strength. Even when the $E1$ contribution is suppressed (in the ^{4}He+^{24}Mg reaction), it exceeds the $E0$ strength by at least two orders of magnitude. The calculated cross section integrated between 15 and 25 MeV for the $E0$ strength is $\sigma(E0)=0.2$ nb, with the chosen parameters of the monopole strength function given in Table I. It is interesting to note the very strong peak due to the decay of the 6.05 MeV 0^+ state in ^{16}O, which is populated by three successive α-particle decays.

III. POSITRON-ELECTRON PAIR SPECTROSCOPY INSTRUMENT

The positron-electron pair spectroscopy instrument (PEPSI) has been designed for studying the emission of positron-electron pairs in the total transition energy range of about 10–40 MeV [23]. Since the cross sections are only in the order of nanobarns (see Sec. II B), excellent background reduction and a large solid angle are imperative. In order to distinguish different multipolarities it is necessary to measure the angular opening between the positron and the electron, as well as their individual momenta. Based on these considerations we have built a novel 4π magnetic filter consisting of strong permanent magnets. This compact structure selects and focuses electrons and positrons with energies above 5 MeV into a multidetector system of 32 plastic scintillators: 12 for e^+ and 20 for e^-. For each detector the magnetic filter resembles an individual miniorange spectrometer [32–34]. The complete spectrometer is shown in Fig. 4.

The magnetic filter of PEPSI was constructed from a new

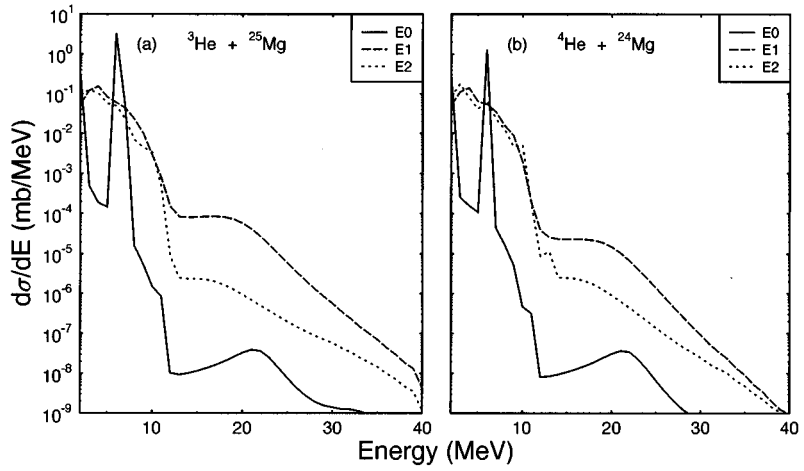

FIG. 3. Dilepton yields calculated with a modified version of CASCADE (see text), for the decay of ^{28}Si populated at an initial excitation energy of 50 MeV, for two different reactions. The solid line represents the $E0$ yields, the dashed line the $E1$ yields and the dotted line the $E2$ yield.

type of ferromagnetic material, $Nd_2Fe_{14}B$, which has a high remnant magnetic induction B_r of 1.1 to 1.3 T. The magnetic field strength in each magnetic gap ranges between 0.3 and 0.5 T. There are 32 (20+12) cylindrical ($\varnothing$30×60 mm) absorbers made of heavy metal (mainly tungsten) for efficient shielding of γ rays emitted from the target. The 4π magnetic filter (Fig. 4) has an outer diameter of approximately 40 cm. The magnetic filter and the detectors are kept under vacuum.

The design and transmission characteristics of PEPSI are extensively discussed elsewhere [23]. The e^+ and e^- particles emitted from the target, placed at the geometrical center of PEPSI, are transmitted through a magnetic gap onto a specific detector, where their individual energies are measured. The novel and essential feature of PEPSI is that each miniorange filter of a specific charge (i.e., e^+) is surrounded by the opposite charged (e^-) minioranges. With PEPSI the two leptons can be detected with opening angles ranging from 0° (both particles entering the same magnetic gap) up to 180°. Nearest-neighbor detectors, all at a relative angle of 37.4° include detection of 0° pairs. Other (average) detection angles are found at 79.2°, 100.8°, and 142.6° (which also includes 180° detection), respectively. The angular resolution is determined by the acceptance of each magnetic gap and therefore each particular pair of detectors reflects a certain angular range. The absolute efficiency of PEPSI for isotropically emitted electrons (positrons) deduced from our measurements [23] peaks at 20% (30%) around 6–7 MeV per particle and decreases to one-third of the peak value at 12 MeV (see Fig. 5).

The ^{12}C$(p,p')^{12}$C* reaction at an incident beam energy of 20 MeV was used at the beginning and end of the ^{28}Si* experiment in order to calibrate the energy and efficiency of both the e^+e^- and the γ-ray spectrometers used. This reaction populates strongly the 15.1 MeV $J^\pi=1^+$, $T=1$ state in ^{12}C, which then decays to the ground state by an $M1$ transition with a measured cross section for photon emission of σ_γ=8.2 mb [35]. The dominant electromagnetic decay channel is the photon decay; at this energy the calculated branching ratio for decay by internal pair conversion in the Born approximation is [1] α_π(15.1 MeV, $M1$)=3.0×10^{-3}. The pair decay of the 15.1 MeV level of ^{12}C was studied before [36], but no experimental α_π value was reported. Typical proton beam currents of 40 particle nA were used to bombard a 2 mg/cm^2 thick target. The e^+e^- decay and the

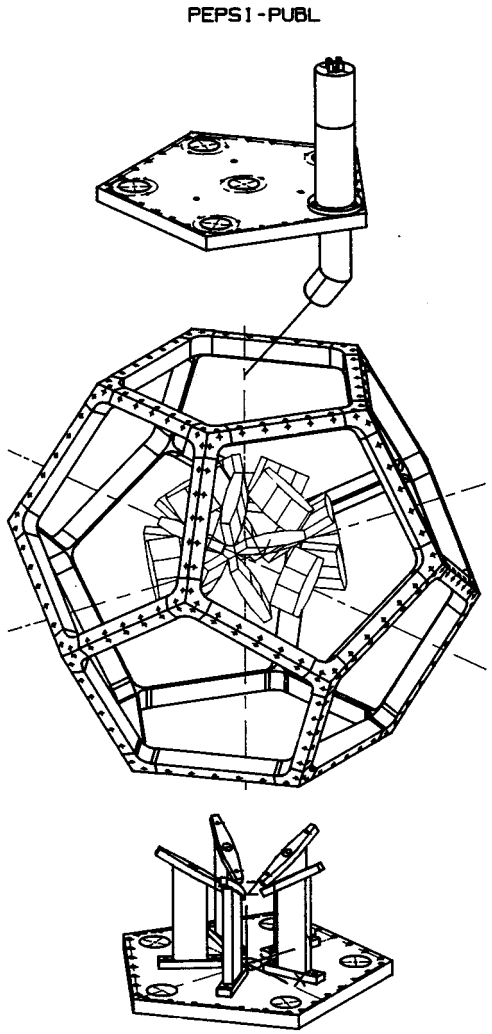

FIG. 4. Schematic drawing of the dilepton spectrometer PEPSI, and its vacuum chamber. Two (of the 12) flanges of the vacuum chamber showing how the detectors are held in place, are also drawn. The 4π magnetic filter can be seen in the center of the vacuum chamber.

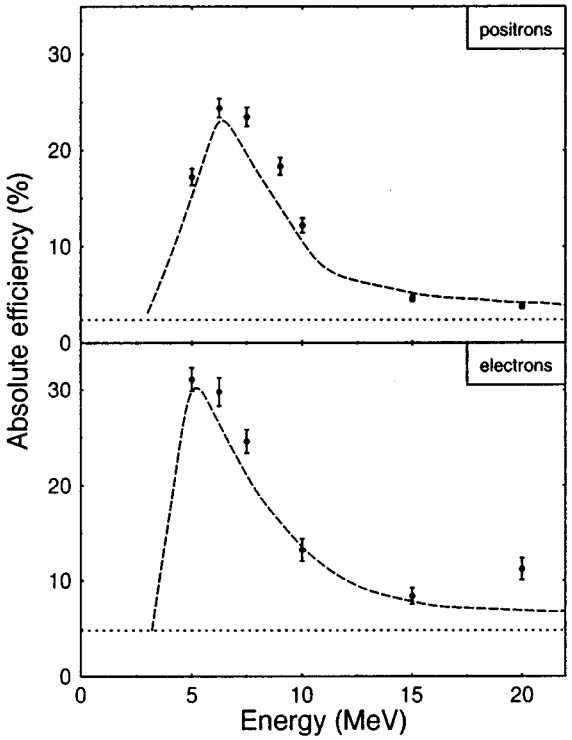

FIG. 5. Efficiency of PEPSI for isotropically emitted positrons and electrons. The experimentally measured points were obtained using electrons from an electron accelerator (see [23]). The dashed line represents the Geant calculated response.

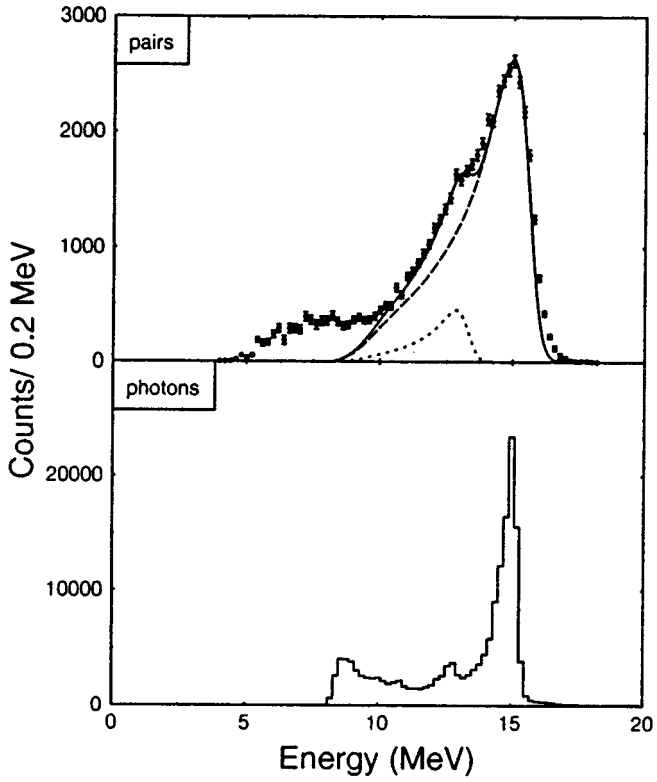

FIG. 7. Measured dilepton and photon spectra for the decay of the 15.1 MeV, $J^{\pi}=1^{+}$ state in ^{12}C. Simulations for the response of PEPSI to 15 and 12 MeV transitions via dilepton decays are shown as dashed and dotted lines, respectively.

photon-decay processes were measured simultaneously by PEPSI and a large NaI(Tl) spectrometer with a known efficiency [37]. The latter was positioned at an angle of 108° with respect to the beam direction (at this angle the suppression of γ rays by all material of PEPSI is minimal) and at a distance of 152 cm from the target position, where it subtended a solid angle of 4.1 msr. The NaI(Tl) crystal was surrounded by a plastic-scintillator shield. This shield was used in anticoincidence with the central crystal to reject cosmic-ray events and compton scattered events.

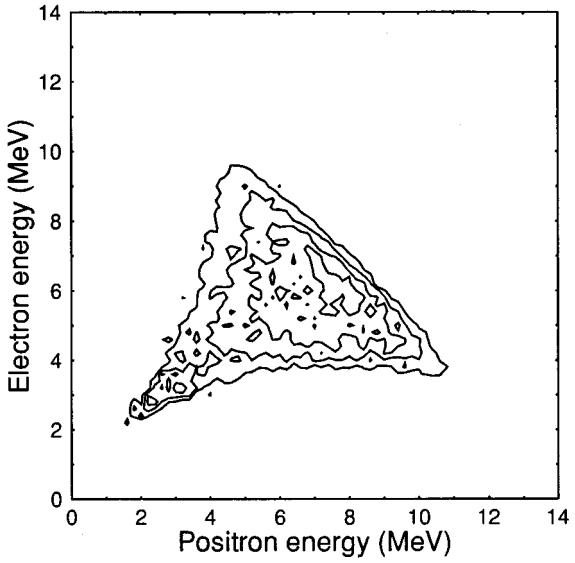

FIG. 6. Two-dimensional spectrum of electron vs positron energy for the decay of the 15.1 MeV, $J^{\pi}=1^{+}$ state in ^{12}C, populated via the ^{12}C$(p,p')^{12}$C* reaction at $E_p=20$ MeV. Contour lines are separated by 40 counts.

The final background subtracted e^+e^- energy matrix for $0°<\theta_{e^+e^-}<60°$ is shown in Fig. 6. In this figure one can clearly see the characteristic ''ridge'' perpendicular to the diagonal (i.e., representing events with a constant $E_{e^+}+E_{e^-}$) and corresponding to the full energy deposit in the positron and electron detectors for the 15.1 MeV transition. The e^+e^- total-energy ($E_{e^+}+E_{e^-}+2m_ec^2$) spectrum together with the measured photon spectrum is shown in Fig. 7. With the known efficiency of the NaI(Tl) spectrometer [37] and of PEPSI [23], it was possible to determine the experimental value of $\alpha_\pi(15.1\ \text{MeV}, M1)=(3.2\pm0.2)10^{-3}$, which is in good agreement with the calculated value in the Born approximation. The experimental error quoted include both statistical and systematic errors. The Born approximation gives as well a good description of the measured energy sharing between the positron and electron for the 15.1 MeV transition, as shown in Fig. 8. In order to eliminate systematic errors from the final uncertainties for the in-beam studies of ^{28}Si*, the ratio between the measured dilepton and photon yields for the 15.1 MeV transition is taken to represent the calculated value of $\alpha_\pi(15.1\ \text{MeV}, M1)=3.0\times10^{-3}$.

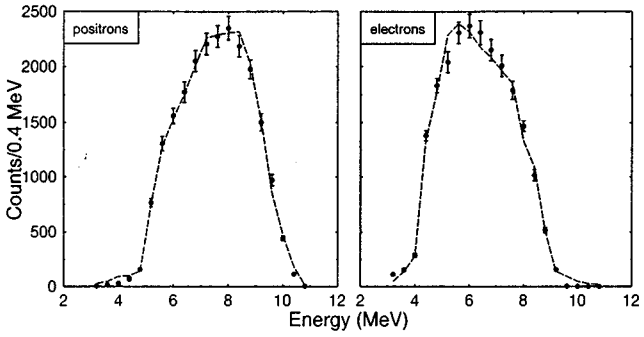

FIG. 8. Energy sharing between the positron and the electron, for the decay of the 15.1 MeV, $J^{\pi}=1^{+}$ state in ^{12}C. The dashed curves represent the measured γ-ray yield at 15.1 MeV, "converted" into $e^{+}e^{-}$ yields in the Born approximation.

IV. EXPERIMENTAL DILEPTON YIELD FROM ^{28}Si*

Two consecutive experiments were performed at the KVI using the $K=160$ AVF cyclotron. In the first one, a ^{24}Mg target was bombarded by ^{4}He ions with an energy of 48 MeV, whereas in the second one a 31 MeV ^{3}He beam bombarded a ^{25}Mg target. The projectile energies were chosen in such a way that both reactions formed the ^{28}Si compound nucleus at an excitation energy of 50 MeV in the middle of the target. The targets were 99.5% enriched and had thicknesses of 15.5 mg/cm^2 and 18.5 mg/cm^2, respectively. The measurements were performed with beam currents of about 10 pnA. Under such experimental conditions PEPSI with its high selectivity for $e^{+}e^{-}$ events is essential since other radiation processes produced at the target have a much larger yield.

In each of the two experiments, both the $e^{+}e^{-}$ pairs and the γ rays were measured simultaneously by PEPSI (see Sec. III) and by a large NaI(Tl) spectrometer [37], respectively.

The count rate above an energy threshold of 0.5 MeV for the plastic-scintillator detectors of PEPSI was 10–20 kHz per detector. The energy thresholds for the data acquisition trigger were set at 2.5–3 MeV, which resulted in a count rate of about 1 kHz per detector. This corresponded to 300 Hz coincidence rate between all (12) positron and all (20) electron detectors. The NaI(Tl) detector with a low threshold ($E_{\gamma}\geqslant 1$ MeV) was counting at the rate of 70 kHz and with a high threshold ($E_{\gamma}\geqslant 8$ MeV) at 300 Hz.

The measured photon spectrum for the ^{3}He+^{25}Mg and the ^{4}He+^{24}Mg reactions are shown in Fig. 9. Absolute γ-ray cross sections were determined from the detected number of photons, making use of the known target thicknesses, accumulated charge (corrected for losses between the target and the Faraday cup), solid angle of the NaI(Tl) crystal and γ-ray detection efficiency. This procedure allowed for a determination of the absolute cross sections with an accuracy of about 20%. The absolute γ-ray cross section for the ^{3}He+^{25}Mg reaction is about five times larger than that observed for the ^{4}He+^{24}Mg reaction (see Fig. 9), for $E_{\gamma}\geqslant 12$ MeV.

The measured γ-ray yields are compared with those obtained by calculations using the CASCADE code (solid lines in Fig. 9). The parameters used in these calculations were discussed in Sec. II. The CASCADE calculations reproduce rather well the measured spectra up to an energy of about 22 MeV,

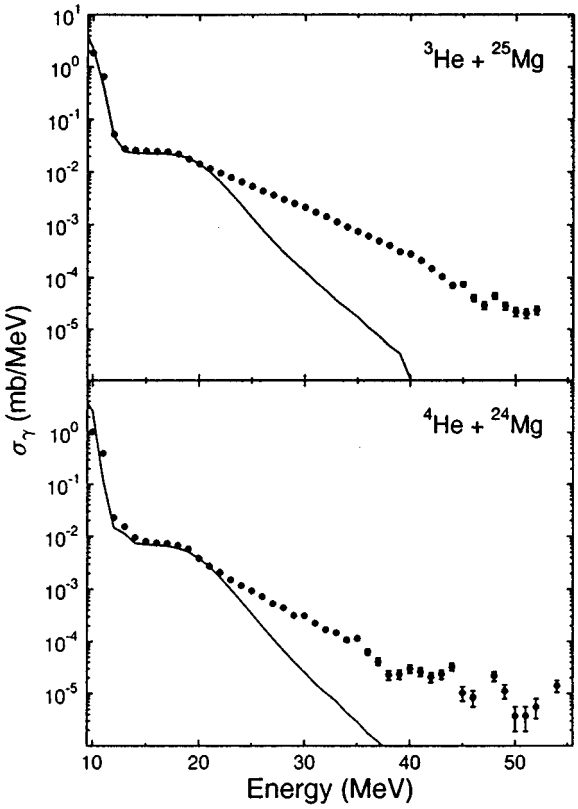

FIG. 9. Measured photon spectra for ^{28}Si, populated at an initial excitation energy of $E^{*}=50$ MeV, in both reactions studied. The solid line represents CASCADE calculations discussed in the text.

even in absolute values. The extra strength measured at $E_{\gamma}>22$ MeV, indicates that in these experiments nonstatistical processes, such as preequilibrium excitations or proton-neutron bremsstrahlung, are playing a dominant role [28,38].

Figure 10 illustrates the analyses of the $e^{+}e^{-}$ data performed for the ^{4}He+^{24}Mg reaction. In this figure four two-dimensional (2D) matrices of $E_{e^{+}}$ versus $E_{e^{-}}$ are shown for the data set with the smallest positron-electron opening angle $\theta_{e^{+}e^{-}}<60°$. To exclude any influence from, e.g., forward-angle-scattered beam particles, only the data set corresponding to the backward hemisphere with respect to the beam direction was considered in the results presented here. Moreover, detectors which might be in particular exposed to different kinds of background (e.g., those positioned closest to the beam entrance of PEPSI) were not included in the data analysis.

The four matrices shown in Fig. 10 were obtained for different conditions in the event time structure. Random coincidences [Fig. 10(b)], and cosmic-ray contributions [Fig. 10(c)] are shown as well as the prompt coincidence data [Fig. 10(a)]. The random and cosmic-ray background subtracted data set are shown in the panel labeled "true" [Fig. 10(d)]. Positron-electron energy matrices for larger $\theta_{e^{+}e^{-}}$ ranges, and from the reaction ^{3}He+^{25}Mg have analogous structure.

A detailed examination of the background-subtracted positron-electron energy matrices revealed that a significant contribution to the dilepton yield for a total energy above 20

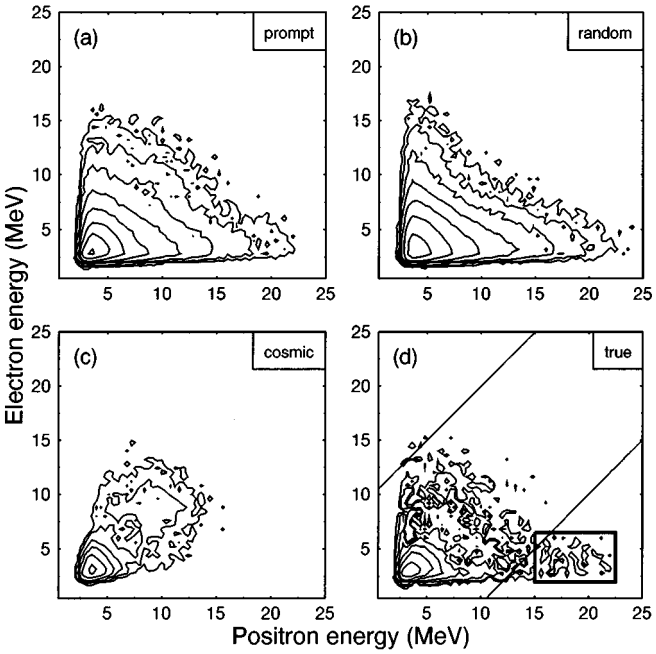

FIG. 10. Two-dimensional spectra of positron vs electron energy for different conditions on the event time structure, for the ^{4}He+^{24}Mg data set, for the smallest dilepton opening-angle range ($\theta_{e^+e^-}<60°$). The solid lines parallel to the diagonal in (d) represent a corridor of $|E_{e^+}-E_{e^-}|<10$ MeV.

MeV was associated with a low (4–6 MeV) energy deposit in the electron detector. This region is indicated in Fig. 10(d) by a rectangle. No transition of the types under consideration (e.g., $E0$, $E1$, $E2$, or $M1$) gives this kind of response in our detection system. This feature, although not understood, seems to have about the same intensity (within statistical errors) in the two reactions and was found to have a flatter opening-angle ($\theta_{e^+e^-}$) distribution. As its origin is not clear, it was decided to exclude this region in the further data analysis by applying a two-dimensional gate $|E_{e^+}-E_{e^-}| \leqslant 10$ MeV [solid lines parallel to the main diagonal in Fig. 10(d)] on the measured e^+e^- energy matrices. The same gate was applied to the e^+e^- energy matrices calculated from the measured γ spectra. This cut is justified since the energy sharing of the dileptons is otherwise well understood. Figure 11 shows energy sharing spectra for our data at two different total energies for both reactions studied. As it can be seen the expected energy sharing (dashed lines in the figure) as calculated from the IPC of the measured γ-ray yields in the Born approximation, describe the data rather well within the chosen "corridor," $|E_{e^+}-E_{e^-}| \leqslant 10$ MeV.

The total-energy ($E_{e^+}+E_{e^-}+2m_ec^2$) spectra corresponding to the matrices shown in Fig. 10 are presented in Fig. 12. One can clearly see the importance of the background subtraction. At $E_{e^+e^-}\approx 20$ MeV, the ratio of prompt to random events is about two.

The background subtracted total-energy e^+e^- spectra obtained from our analyses are shown in Fig. 13 for both reactions. The measured photon yields "converted" into e^+e^- yields using the same $|E_{e^+}-E_{e^-}| \leqslant 10$ MeV energy gate are also shown in this figure as solid lines. The good agreement between the measured and converted e^+e^- yield reflects the

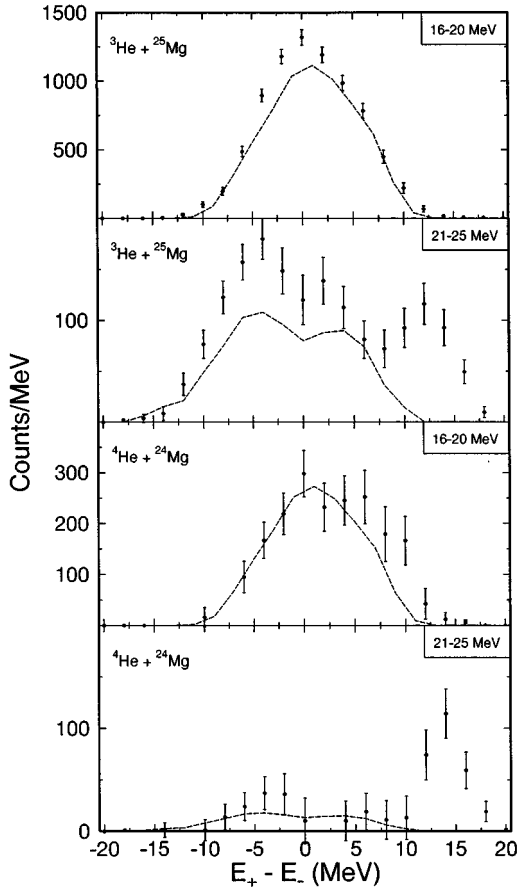

FIG. 11. Measured energy sharing between the positron and the electron for two transition energy ranges in both reactions studied. The dashed curves represent the measured γ-ray yield "converted" into e^+e^- yields in the Born approximation.

fact that by far most of the measured dilepton strength stems from the internal-pair-conversion process of the photon-decay channel indeed. Thus, the Born approximation which was used to fold the measured γ-ray strength with the response of PEPSI provides, within the accuracy of the present experiment, a good description of the energy sharing (see Fig. 11), the different opening-angle ranges studied (see Fig. 13) and of the absolute value of the internal-pair-conversion coefficient. It is worth stressing that there has been no renormalization between the measured e^+e^- yield and the solid lines in Fig. 13. The conversion of measured γ rays into e^+e^- yields is fixed by the 15.1 MeV measurement and the energy dependence of the IPC coefficient $\alpha_\pi(E_\gamma)$ is given by the Born approximation.

An interesting question is whether, within the accuracy of the present data, there is any additional dilepton strength, i.e., an excess of dilepton strength over the one estimated from the measured γ rays. Figure 14 presents the differences between the measured and the "converted" e^+e^- spectra for the four data sets shown in Fig. 13. Any excess strength has to originate from a process which does not give a signature in the photon yield, the most natural "candidate" being the monopole decay. An analysis was performed whereby an $E0$ component was assumed to exist with a strength to be determined by the statistical accuracy of the measured excess data. The data from Fig. 14 can be converted into absolute

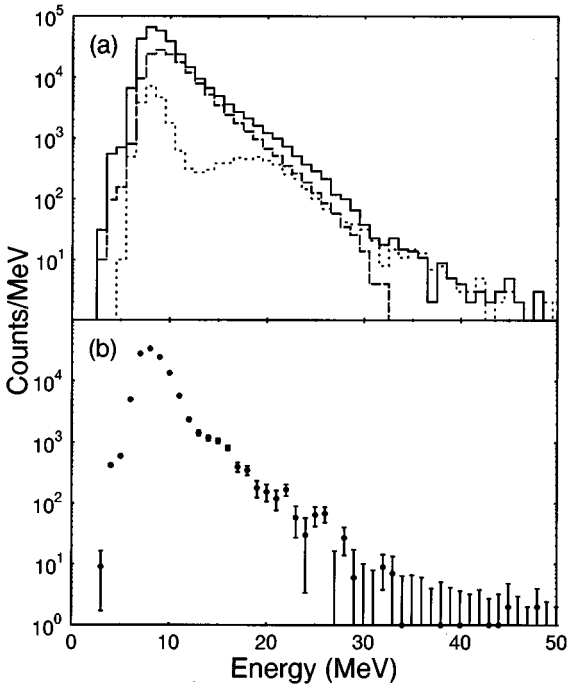

FIG. 12. Total projections of the two-dimensional matrices shown in Fig. 10, onto an axis representing the total transition energy, $E_{e^+}+E_{e^-}+2m_ec^2$ in MeV. The solid, dashed, and dotted histograms are the projections, with the condition $|E_{e^+}-E_{e^-}|<10$ MeV, of the prompt-, random-, and cosmic-ray 2D spectra, respectively. The spectrum shown in the lower panel represents the projection of the ''true'' 2D spectra, i.e., background subtracted data.

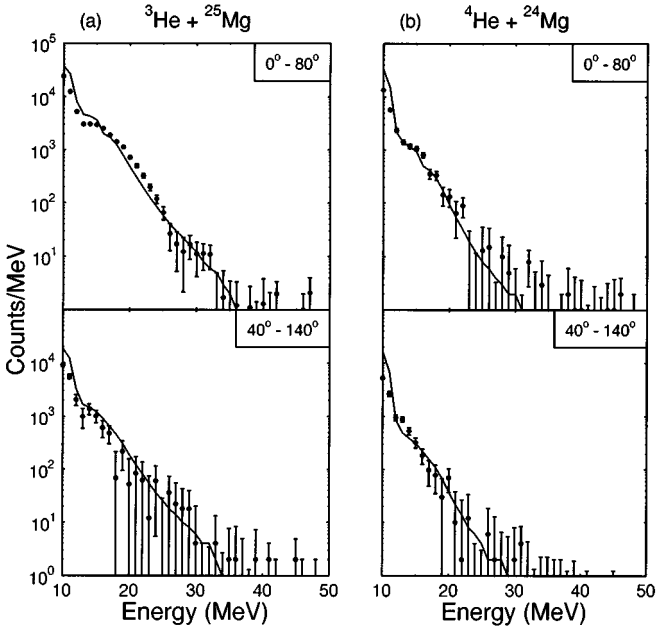

FIG. 13. The dilepton yields for two ranges of opening angles between the electron and positron for ^{28}Si measured in both reactions. The lines represent the measured photon yields, converted into dilepton yields, using the response function of the spectrometers and the Born approximation for the energy dependence of the IPC coefficient $\alpha_\pi(E_\gamma)$.

cross sections by unfolding the response of PEPSI for the transitions of $E0$ type. The following procedure was applied for each of the four data sets. First, the best curve through the data points has been determined. Here, the best curve means a strength distribution which obeys two conditions: (i) it gives the minimum value of chi square ($\chi^2_{\min}$) and (ii) it is greater than or equal to zero at all energies, therefore representing real ''physical'' strength. In the next step, a Monte Carlo method has been used to probe all possible curves which give $\chi^2 \leqslant \chi^2_{\min}+1$ and fulfill condition (ii). The extracted experimental limits for the cross section of a possible $E0$ dilepton strength, integrated over the energy range 17–30 MeV, are presented in Table II. The $E0$ e^+e^- yield calculated by CASCADE for the decay of excited nuclear states in ^{28}Si at $E^*=50$ MeV, integrated over the same energy range, is about 0.2 nb (see Fig. 3). It is practically equal for the two reactions as the main contribution to it comes from the ISGMR (see Sec. II B). Such a low cross section for monopole pair emission falls within the experimentally determined limits for the two data sets of the ^{4}He induced reaction. In fact, because of the relatively low statistical accuracy of the experimental ^{4}He+^{24}Mg data, one can only estimate a 1σ upper limit of 3 nb (see Table II). The data for the ^{3}He+^{25}Mg reaction for the largest $\theta_{e^+e^-}$ range, are consistent with this upper limit. However, the data set for $0°<\theta_{e^+e^-}<60°$ in the ^{3}He+^{25}Mg reaction shows, in the energy range 17–30 MeV, a statistically significant excess of counts. This excess, which implies a large cross section of $\sigma(E0)=286^{+100}_{-90}$ nb as given in Table II, is not consistent with the one estimated from the data for larger opening angles [$\sigma(E0)<14$ nb] or with the data for the ^{4}He induced reaction [$\sigma(E0)<3$ nb]. It cannot be explained within the framework of the Hauser-

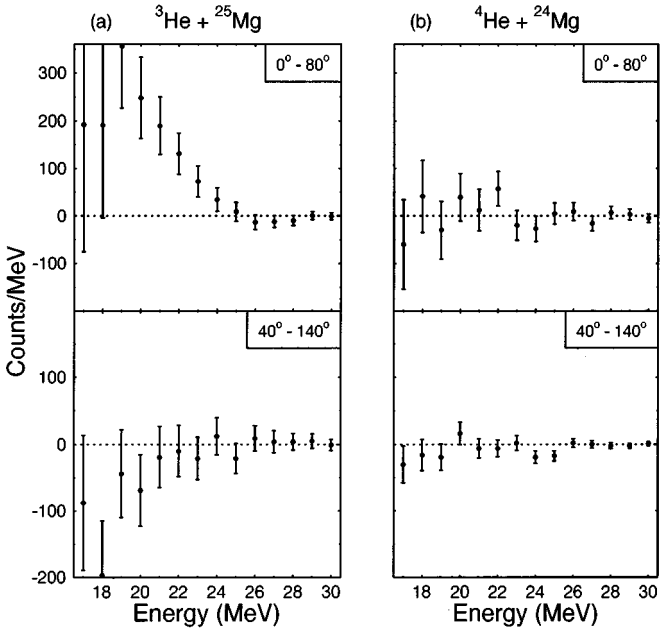

FIG. 14. The difference between the dilepton data and the converted photon yields shown in Fig. 13.

TABLE II. Limits of the excess dilepton cross sections calculated from the data shown in Fig. 14 for $E0$ transition type, integrated over the transition energy region of 17–30 MeV.

Reaction	σ_{E0} (nb) $0°<\theta_{e^+e^-}<60°$	σ_{E0} (nb) $60°<\theta_{e^+e^-}<140°$
^{4}He+^{24}Mg	1^{+15}_{-1}	0^{+3}_{-0}
^{3}He+^{25}Mg	286^{+100}_{-90}	1^{+13}_{-1}

Feshbach statistical model. This puzzling observation implies either that the excess of dilepton strength observed in the ^{3}He induced reaction results from some yet unknown experimental problem or that it is a manifestation of a strong entrance-channel effect.

The physical interpretation of the observed excess yield are restricted to phenomena which would not give any significant contribution to the measured photon yield but would give the extra e^+e^- strength observed in particular for the ^{3}He+^{25}Mg reaction. Assuming the excess to have a dipole character, the following point should be noted: the γ-ray detector was positioned at an angle 108° with respect to the beam direction and the photon yield was ''converted'' into the dilepton yield assuming an isotropic $E1$ photon distribution. This means that an anisotropy of the γ-ray emission at this energy range (19–25 MeV) could, in principle, explain the observed excess of dilepton strength with respect to the measured γ-ray yield. A simple estimate using $W(\theta)=A[1+a_2P_2(\cos\theta)]$ for the anisotropy of γ emission with respect to the beam direction, gives $a_2=+0.9$. This unusually large value of the anisotropy is in disagreement with the measurements for the same reaction performed by Steierwald *et al.* [39] and Behr *et al.* [28], where an almost isotropic γ-ray distribution was reported for this γ-ray energy region.

Another scenario is to consider an entrance-channel effect in the ^{3}He+^{25}Mg reaction which could lead to an extra $E0$ e^+e^- strength, although one should note that the measured excess strength (see Table II) is not consistent with an $E0$ opening angle distribution. For instance, one neutron pickup by ^{3}He could populate the 20.1 MeV 0^+ state in ^{4}He. The subsequent decay of this state to the 0^+ ground state by an $E0$ transition would result in emission of e^+e^- pairs. Note that the experimentally determined cross section to excite this 0^+ state in the ^{24}Mg(α,α*) reaction is very small $\sigma<5$ μb [40]. The calculated distorted wave Born approximation (DWBA) cross section for the ^{25}Mg(^{3}He,α*) reaction populating the 0^+ first excited state in ^{4}He, for ^{3}He energies around 30 MeV is 0.45 mb [40–42]. The 0^+ state is particle unstable and has a total line width of about 270–500 keV [43,44]. Therefore, from the measured $\sigma_{e^+e^-}(E0)=286^{+100}_{-90}$ nb (see Table II) one can deduce the partial decay width via e^+e^- decay for the $0^+(20.1\ \mathrm{MeV})\rightarrow 0^+(\mathrm{g.s.})$ in ^{4}He of $\Gamma_{e^+e^-}=172^{+60}_{-54}$ eV. We note that this value is at least 2 orders of magnitude larger than the one expected from the classical EWSR, assuming all strength to be concentrated in this 0^+ state. Furthermore, this excess strength has been analyzed assuming a pure $E0$ transition which is not in agreement with the measured dilepton opening angle distribution.

V. SUMMARY

Two reactions were used to study the dilepton decay of giant resonances built on excited nuclear states of ^{28}Si. In the isoscalar reaction ^{4}He+^{24}Mg$\rightarrow^{28}$Si*, the isospin of the initial state is constrained to $T=0$. In the other reaction ^{3}He+^{25}Mg$\rightarrow^{28}$Si*, states in ^{28}Si with both $T=0$ and 1 are equally populated. With a beam energy of 48 MeV for ^{4}He and 31 MeV for ^{3}He, these two reactions populate states in ^{28}Si at the same initial excitation energy of 50 MeV. In each of the two experiments, two measurements were performed simultaneously: e^+e^- pairs, using the spectrometer PEPSI and γ rays by a large NaI(Tl) spectrometer.

The measured photon spectra showed the expected suppression of $E1$ yield in case of the $T=0$, ^{4}He+^{24}Mg reaction. The statistical Hauser-Feshbach calculations reproduce the γ spectra for the two reactions up to an energy of about 22 MeV. A large nonstatistical yield was observed above this energy. This extra contribution is probably due to preequilibrium excitations and/or proton-neutron bremsstrahlung. As the photon yield carries information about all strength but $E0$, it was used to estimate the contribution to the observed dilepton yield due to the internal-pair-conversion process.

The resulting dilepton spectra show an overall good agreement with the photon spectra ''converted'' into e^+e^- yields. This agreement reflects the fact that by far most of the measured dilepton strength stems from the internal-pair-conversion process indeed. The Born approximation which was used to fold the measured γ-ray strength with the response of PEPSI, gives a good description of this process. It should be noted that the nonstatistical contribution observed in the γ spectra was found in the dilepton yield as well.

The results of these first experiments aimed at a measurement of the GMR strength built on excited nuclear states, do not show an unequivocal signature of $E0$ yield. Because of low statistical accuracy of the present data, in particular for the ^{4}He+^{24}Mg reaction, one can only set an upper limit for the observed $E0$ yield of 3 nb, which has to be compared to a calculated yield of 0.2 nb.

A large excess of dilepton strength was observed for the data set for small opening angles in the ^{3}He+^{25}Mg reaction, which could indicate a strong entrance-channel effect. A possible scenario which involves a neutron pickup followed by the $0^+(20.1\ \mathrm{MeV})\rightarrow 0^+(\mathrm{g.s.})$ deexcitation of ^{4}He implies a large e^+e^- partial decay width for the 0^+, 20.1 MeV excited state in the α particle. Further experiments should improve the statistical accuracy of the present data and attempt to resolve the ''puzzle'' about the small dilepton opening-angle data from the ^{3}He induced reaction.

ACKNOWLEDGMENTS

This work has been supported by the Stichting Fundamenteel Onderzoek der Materie (FOM) which is financially supported by the Nederlandse Organisatie voor Wetenschapelijk Onderzoek (NWO). It was further complemented by a NATO grant for collaborative research crg920608 and the Polish KBN Project No. 2 0174 91 01.

[1] P. Schlüter, G. Soff, and W. Greiner, Phys. Rep. **75**, 327 (1981).
[2] M. E. Rose, in *Alpha-, Beta- and Gamma-Ray Spectroscopy*, edited by K. Siegbahn (North-Holland Publishing Company, Amsterdam, 1965), Vol. 2, p. 887.
[3] J. Kantele, in *Heavy Ions and Nuclear Structure*, edited by B. Sikora and Z. Wilhelmi (Harward Academic Publications, New York, 1984).
[4] D. H. Wilkinson, Nucl. Phys. A **133**, 1 (1969).
[5] A. van der Woude, in *Electric and Magnetic Giant Resonances*, edited by J. Speth (Word Scientific Publishing Company, Singapore, 1991), p. 99.
[6] J. P. Blaizot, Phys. Rep. **64**, 171 (1980).
[7] J. Treiner, H. Krivine, O. Bohigas, and J. Martorell, Nucl. Phys. A **371**, 253 (1981).
[8] A. van der Woude, Prog. Part. Nucl. Phys. **18**, 217 (1987).
[9] M. M. Sharma, W. T. A. Borghols, S. Brandenburg, S. Crona, A. van der Woude, and M. N. Harakeh, Phys. Rev. C **38**, 2562 (1988).
[10] M. N. Harakeh, B. van Heyst, K. van der Borg, and A. van der Woude, Nucl. Phys. **A327**, 373 (1979).
[11] Y.-W. Lui, J. D. Bronson, D. H. Youngblood, Y. Toba, and U. Garg, Phys. Rev. C **31**, 1643 (1985).
[12] S. Brandenburg, W. T. A. Borghols, A. G. Drentje, L. P. Ekström, M. N. Harakeh, A. van der Woude, A. Håkanson, L. Nilsson, N. Olsson, M. Pignanelli, and R. De Leo, Nucl. Phys. **A446**, 29 (1987).
[13] D. Brink, Ph.D. thesis, Oxford University, 1955, unpublished; Nucl. Phys. **A482**, 3c (1988).
[14] K. A. Snover, Annu. Rev. Nucl. Part. Sci. **36**, 545 (1986).
[15] J. J. Gaardhøje, Annu. Rev. Nucl. Part. Sci. **42**, 483 (1992).
[16] I. Bombaci, T. T. S. Kuo, and U. Lombardo, Phys. Lett. B **331**, 9 (1993).
[17] C. P. Montoya, S. Schadmand, L. Diószegi, D. J. Hofman, P. H. Zhang, and P. Paul, Z. Phys. A **340**, 371 (1991).
[18] S. Schadmand, R. Varma, S. R. Banerjee, B. B. Back, D. J. Hofman, C. P. Montoya, and P. Paul, J. Phys. G **21**, 821 (1995).
[19] A. Buda, J. C. Bacelar, A. Balanda, Z. Sujkowski, A. van der Woude, R. Bersch, H. Ching, I. Dioszegi, D. J. Hofman, P. Paul, S. Schadmand, and R. Varma, Phys. Rev. Lett. **75**, 798 (1995).
[20] A. Buda, J. C. Bacelar, A. Balanda, H. van der Ploeg, Z. Sujkowski, and A. van der Woude, Nucl. Phys. A **553**, 509c (1993).
[21] J. C. Bacelar, A. Buda, A. Balanda, A. Krasznahorkay, H. van der Ploeg, Z. Sujkowski, and A. van der Woude, Nucl. Phys. **A569**, 101c (1994).
[22] F. Pühlhofer, Nucl. Phys. **A280**, 267 (1977).
[23] A. Buda, J. C. Bacelar, A. Balanda, J. van Klinken, Z. Sujkowski, and A. van der Woude, Nucl. Instrum. Methods A **335**, 479 (1993).
[24] M. N. Harakeh, D. H. Dowell, G. Feldman, E. F. Garman, R. Loveman, J. L. Osborne, and K. Snover, Phys. Lett. B **176**, 297 (1986).
[25] A. Bohr and B. R. Mottelson, *Nuclear Structure* (Benjamin, New York, 1975), Vol. 2.
[26] N. Auerbach, J. Phys. **45**, C4 (1984).
[27] Ch. Hofmann, J. Reinhardt, W. Greiner, P. Schlüter, and G. Soff, Phys. Rev. C **42**, 2632 (1990).
[28] J. A. Behr, K. A. Snover, C. A. Gossett, M. Kicińska-Habior, J. H. Gundlach, Z. M. Drebi, M. S. Kaplan, and D. P. Wells, Phys. Rev. Lett. **70**, 3201 (1993).
[29] A. Erell, J. Alster, J. Lichtenstadt, M. A. Moinester, J. D. Bowman, M. D. Cooper, F. Irom, H. S. Matis, E. Piazetsky, U. Sennhauser, and O. Ingram, Phys. Rev. Lett. **52**, 2134 (1984).
[30] F. Irom, J. D. Bowman, G. O. Bolme, E. Piasetzky, U. Sennhauser, J. Alster, J. Lichtenstadt, M. A. Moinester, J. N. Knudson, S. H. Rokni, and E. R. Siciliano, Phys. Rev. C **34**, 2231 (1986).
[31] Y. Toba, Y.-W. Lui, D. H. Youngblood, U. Garg, P. Grabmayr, K. T. Knöpfle, H. Riedesel, and G. J. Wagner, Phys. Rev. C **41**, 1417 (1990).
[32] J. van Klinken and K. Wisshak, Nucl. Instrum. Methods **98**, 1 (1972).
[33] J. van Klinken, S. J. Feenstra, K. Wisshak, and H. Faust, Nucl. Instrum. Methods **130**, 427 (1975).
[34] J. van Klinken, A. Balanda, J. M. Hoogduin, H. Kaper, W. J. Meiring, H. Bokemayer, F. W. N. de Boer, D. Kraft, and K. E. Stiebing, Nucl. Instrum. Methods A **320**, 508 (1992).
[35] D. Berghofer, M. D. Hasinoff, R. Helmer, S. T. Lim, D. F. Measday, and K. Ebisawa, Nucl. Phys. A **263**, 109 (1976).
[36] J. M. Enagonio, F. P. Calaprice, R. W. Dunford, and M. M. Lowry, Phys. Rev. C **25**, 1047 (1982).
[37] H. J. Hofmann, Ph.D. thesis, Rijksuniversiteit Groningen, 1991; H. J. Hofmann, J. C. Bacelar, M. N. Harakeh, T. D. Poelhekken, and A. van der Woude, Nucl. Phys. A **571**, 301 (1994).
[38] A. Balanda, J. C. S. Bacelar, E. Betak, J. A. Bordewijk, AA. Krasznahorkay, H. van der Ploeg, R. H. Siemssen, H. W. Wilschut, and A. van der Woude, Nucl. Phys. A **575**, 348 (1994).
[39] D. Steierwald (private communication); D. Mayer, W. Dünnweber, W. Hering, M. Herrlein, D. Konnerth, S. Kovats, and M. Siemaszko, Annual Report, Beschleunigerlaboratorium der LMU und der TU München (1990), p. 11.
[40] J. van Driel, M. N. Harakeh, R. Kamermans, and R. J. de Meijer, Phys. Rev. Lett. **46**, 525 (1981).
[41] D. Dehnhard and C. Mayer-Bricke, Nucl. Phys. **A97**, 164 (1967).
[42] B. Brinkmöller, H. P. Morsch, P. Decowski, M. Rogge, R. Siebert, and P. Turek, Phys. Rev. C **42**, 550 (1990).
[43] S. Fiarman and W. E. Meyerhof, Nucl. Phys. **A206**, 1 (1973).
[44] D. R. Tilley, H. R. Weller, and G. M. Hale, Nucl. Phys. **A541**, 1 (1992).